

DYNAMIC EVALUATION OF A NEW DEVICE FOR RESPIRATORY PHYSIOTHERAPY

F.P. Lépore Neto*

L.C. de Lima*

A. C. Gastaldi **

*Departamento de Engenharia Mecânica

Universidade Federal de Uberlândia, CEP 38400 902 Uberlândia MG, Brazil

**UNIT – Centro Universitário do Triângulo

Uberlândia MG – Brazil

***Abstract.** The new device for respiratory physiotherapy known as Flutter resembles a whistle under the form of a smoke-pipe with a 28-g stainless steel sphere inside its conical cavity. Due to the air pressure during the expiration the sphere will vibrate intermittently. This process stimulates “bronchial percussion” which eases sputum elimination. The objectives of the present article are to mechanically characterize the dynamic behavior of such device, to monitor and to analyze the vibratory motion of the sphere, the dynamic pressure at the Flutter inlet, under different airflow rates. Numerical simulations of the fluid velocity and pressure fields and floating heights were also made, using a finite element computational model. Results show interesting aspects to professionals in the field and to the optimization of the Flutter’s mechanical design.*

Key words: flutter, floating sphere, characteristic frequencies

1. INTRODUCTION

The VRP1-Desitin[®] device also known, as “Flutter” is a small pocket device designed for the treatment of patients suffering from chronic mucus retention and bronchial collapse. Although being simple in its design the Flutter has been showing encouraging performance when compared to traditional respiratory physiotherapy such as, for example, autogenic drainage (Lindemann, 1992). It is based on oscillations of air in the respiratory tract during expiration. Pressure and flow variations depend on the position of the mouthpiece and effort of breathing.

As shown in “Figure 1”, the Flutter is constituted of a mouth-piece (a), a hard material cone (b), a 28 grams high density stainless steel sphere (c), and a perforated and removable lid (d). It works as follow. Before expiration the sphere closes the conical channel. During

expiration, the instantaneous position of the sphere is resulted from the equilibrium state of its own weight, the cone angle and the pressure of the expired air. After the increase in the pressure, the sphere starts to move, permitting air to flow through the variable area orifice (the expiratory flow in this state is under strong acceleration). After this air pressure falls, the sphere rolls back to its initial position and it blocks the orifice, resulting again in the increase of the pressure. This process stimulates “bronchial percussion” easing the elimination of mucus and saliva and the frequency of this cycle can be adapted to each patient. The oscillation frequency, the air pressure and flow depend on the angle position of the mouth-piece and lid of the device as well on the expiration effort.

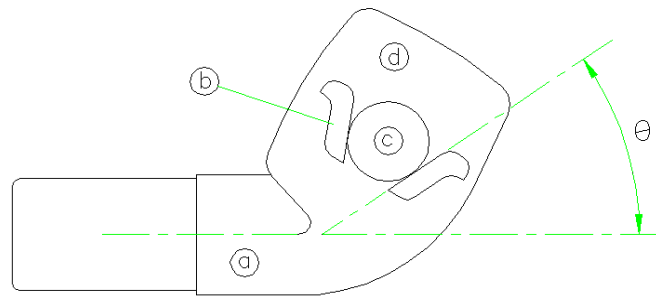


Figure 1. The Flutter device.

The device was submitted to two kinds of verification. The first one was the formulation of a numerical study of the flow through the flutter using the finite element Computational Fluid Dynamics (CFD) ANSYS 5.2TM code, in order to calculate the aerodynamic force acting on the sphere. The second one was the experimental observation of the behavior of the flutter through the measurements of the sphere vibratory motions inside the lid, the air flow rate, and the inlet pressure.

2. MATHEMATICAL AND COMPUTATIONAL MODEL

The Flutter computational model was built using the finite element method to calculate the numerical simulations of the steady state flow developed at the inlet and outlet ducts and at the region around the sphere. The fluid is the air with physical properties independent of the temperature. The package ANSYS 5.2 through its module of Computational Fluid Dynamics named FLOTRAN was used, considering the $K - \epsilon$ model of turbulence, developed by Launder and Spalding (1974). The elements are quadrilateral (FLUID171) and the model is axisymmetric in the X direction. The boundary conditions impose zero velocities at the inner walls and at the sphere surface. The velocity in the Y direction is considered equal to zero on the axisymmetric axis. To simulate a $2.0 \text{ m}^3/\text{h}$ flow, the inlet velocity in the X direction is $V_{in} = 7.13 \text{ m/s}$. At the outlet, the atmospheric pressure is imposed.

The grid is denser at the central region of the model, where the sphere is close to the conical wall, to achieve numerical convergence of the solution, after 60 iterations.

Statically positioning the sphere at 23 different locations on the X direction, the velocity field and the pressure distribution were determined. The “Figure 2 and 3” show the results for some of the sphere positions. Only half of the cross-longitudinal section grid of the Flutter is shown, considering that X is horizontal and $x = 0$ corresponds to the condition of flow obstructed by the sphere.

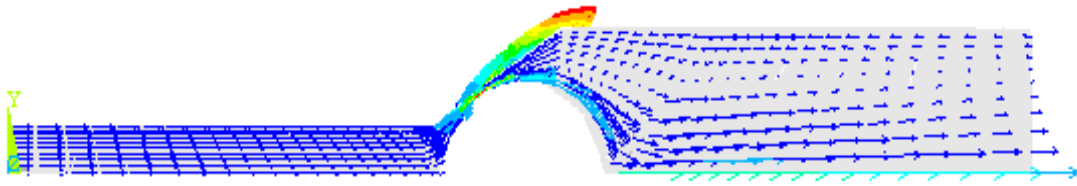


Figure 2. Velocity field: complete model for $V_{in} = 7.13$ m/s and $x = 0.5736$ mm.

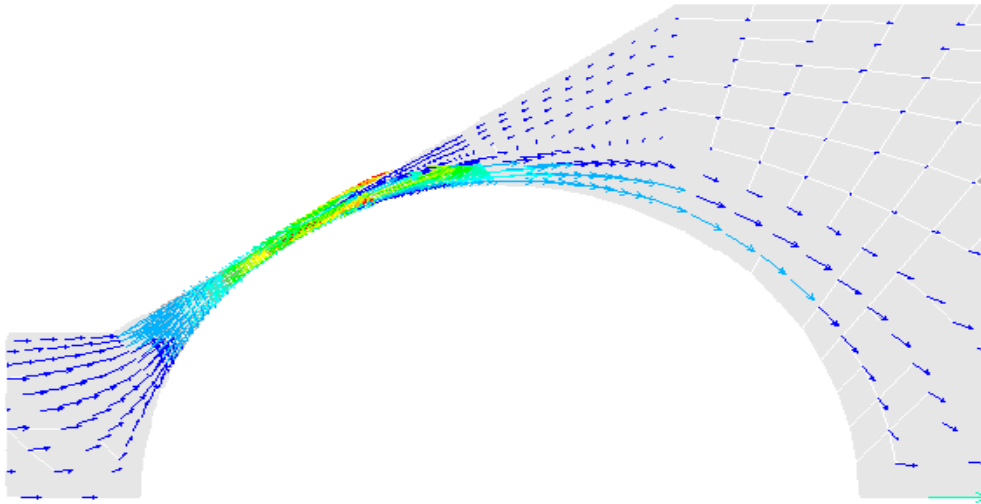


Figure 3. Velocity field: region around the sphere, for $V_{in}=7.13$ m/s and $x = 0.5736$ mm.

The pressure distribution at the model central region is shown, for the same conditions of “Figure 4”, but for $x = 1.3736$ mm that corresponds to a greater orifice area. The maximum pressure of 9902 Pa is in front of the sphere. The pressure is negative at the region where the sphere is close to the conical wall. A vortex formation is present at the right side of the sphere, what can be verified by the pressure negative value of -2000 Pa. This effect can also be observed in the velocity vectors distribution shown in “Figure 1”, although the airflow rate for this situation is relatively small.

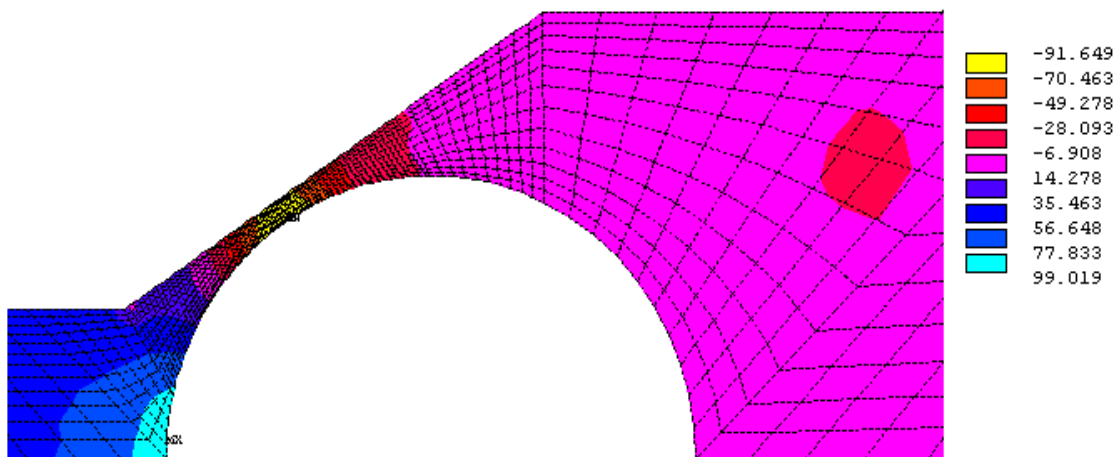


Figure 4. Pressure distribution (x 100 Pa) on the central region of the model, for $V_{in} = 7.13$ m/s and $x = 1.3736$ mm.

The pressure distribution on the sphere is obtained by selecting the model nodes on its surface. The next figure shows one of these distributions, where the frontal position is at the right side that corresponds to an angular position $\theta = 0$ degrees.

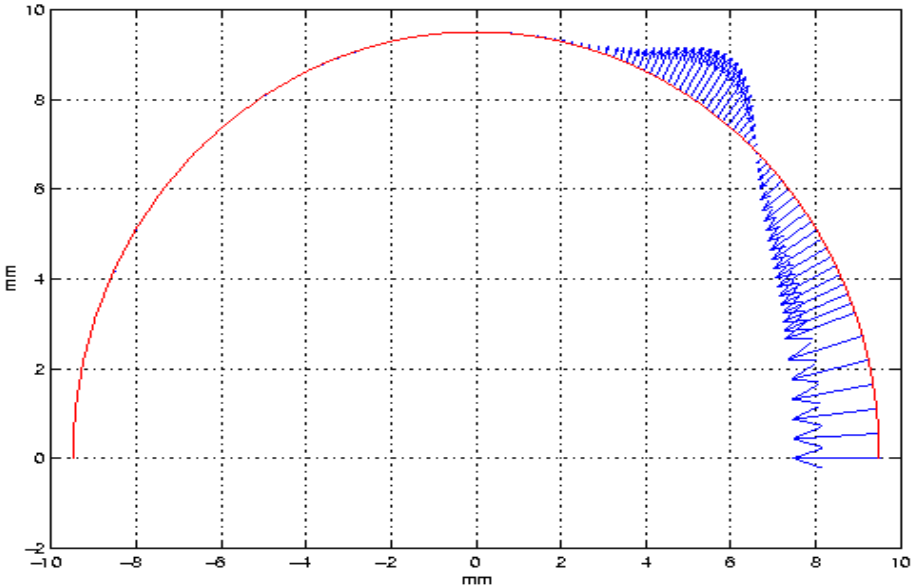


Figure 5. Pressure distribution on the sphere $P(\theta)$, for $V_{in} = 7.13 \text{ m/s}$ and $x = 0.5736 \text{ mm}$.

The lift forces acting on the sphere are calculated by the integrating the pressure distributions obtained for each sphere position x , varying from 0.1736 to 2.5 mm, at steps equal to 0.1 mm. In “Figure 6”, the solid line is the mathematical function fitted to the numerical data by a least square procedure, with mean error of $1.342 \cdot 10^{-5}$. When x is less than 0.1736 mm, the finite element model does not converge because the element geometry is strongly distorted, increasing the numerical errors.

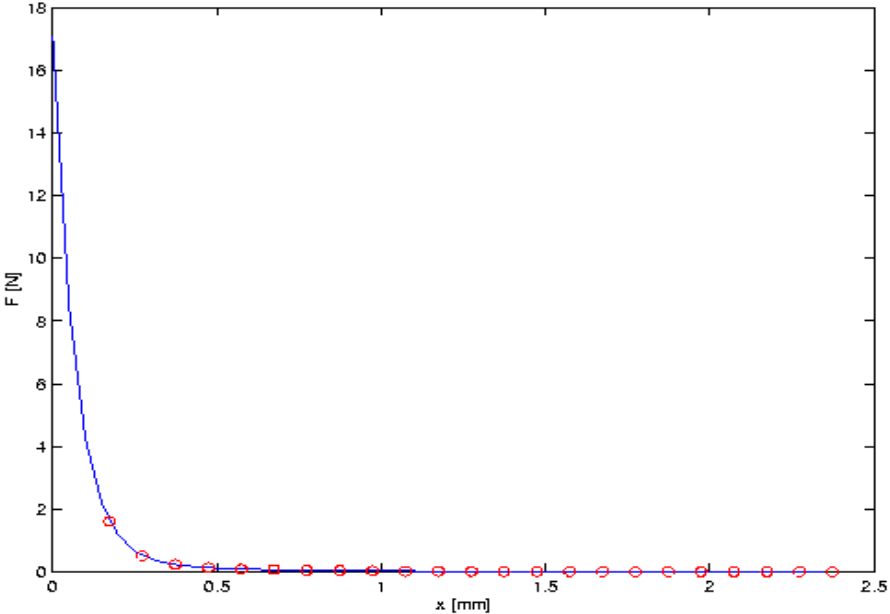


Figure 6. Lift force as a function of the sphere position over X , for $V_{in} = 7.13 \text{ m/s}$.

A further refinement of the grid is not computationally feasible because of the huge processing time involved to obtain the solution. So, the lift aerodynamic force model can not be used to calculate the sphere vibrations for displacements less than 0.1736 mm, but this model can be used to extrapolate force values for x greater than 2.5 mm, considering that $F(x)$ has a smooth variation for greater values of x

To evaluate the vibratory motion of the sphere a simplified one degree of freedom dynamic model was assumed, as shown in “Figure 7”, where the X direction is vertical, the forces on the sphere are the aerodynamic, $F(x)$, and the gravitational, mg .

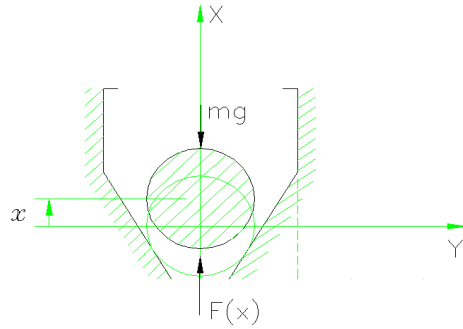


Figure 7. Dynamic model of the Flutter in the vertical position

The mathematical model is presented in “Equation 1”, where m is the sphere mass, g is the acceleration of gravity, and $F(x)$ is the nonlinear aerodynamic lift force. For $V_{in} = 7.13$ m/s, the function that describes $F(x)$ has the following parameters: $c_1 = 16.635$ N, $c_2 = 0.473$ N, $\lambda_1 = 14573$ m⁻¹ and $\lambda_2 = 3054$ m⁻¹. This equation is solved numerically by a 4th order Runge-Kutta method, using a time step $dt = 0.5$ ms. The steady state vibratory motion, is shown in “Figure 8” where only the last 2048 data points are plotted.

$$m \ddot{x} = F(x) - mg$$

$$F(x) = c_1 e^{-\lambda_1 x} + c_2 e^{-\lambda_2 x} \quad (1)$$

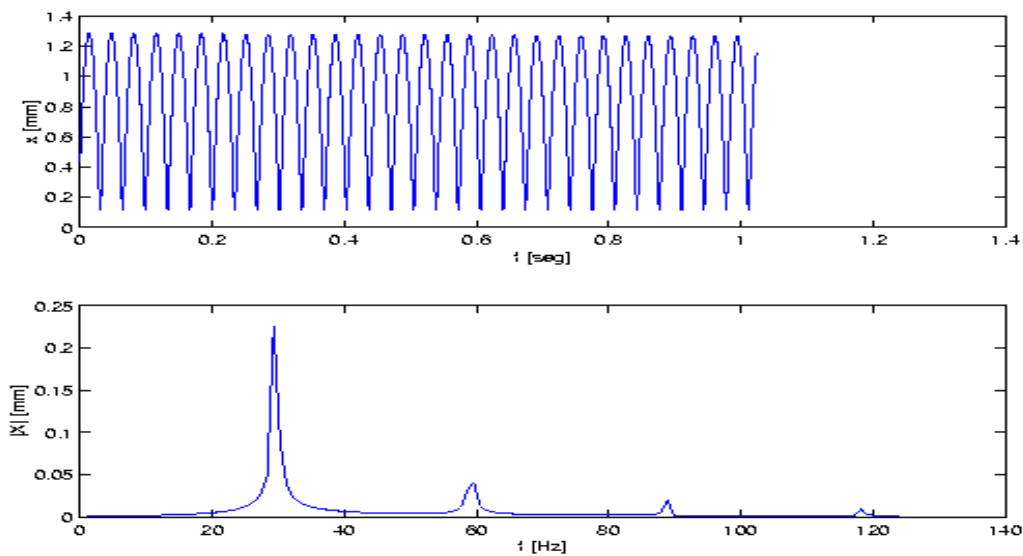


Figure 8. Dynamic model simulation results: $x(t)$ and $|X(f)|$ for $V_{in} = 7.13$ m/s.

The sphere displacement has a mean value equal to 0.625 mm and maximum value of 4.72 mm that occurs just at the beginning of the sphere transient motion. The time domain signal $x(t)$ has periodic characteristic and the velocity presents strong variations when the sphere is almost obstructing the flow. This behavior is in accordance with the fact that the aerodynamic lift force in that position is maximum and decreases exponentially with x . The spectrum has resolution $df = 0.9765$ Hz and shows a fundamental frequency $f_p = 29.3$ Hz.

3. EXPERIMENTAL PROCEDURE

The experimental set up is shown in “Figure 9”. A mechanical compressor feeds air to the Flutter. An inductive proximity transducer, which is linked to a signal conditioner system, measures the vertical movement of the sphere. The proximity transducer has a global static sensitivity of 2.156 V/mm and a 2.5 mm full scale. Air pressure is measured by a piezoelectric transducer which is coupled to a 500 gain voltage amplifier and has static sensitivity of 9167 Pa/V. Airflow rate in the entrance of the Flutter is measured by a calibrated rotameter with the operation range between 1.5 and 16 m³/h. Airflow rates are controlled by a valve. A Signal Analyser acquires time signals of the sphere position and pressure in the entrance tube of the Flutter and data are subsequently transferred to a microcomputer.

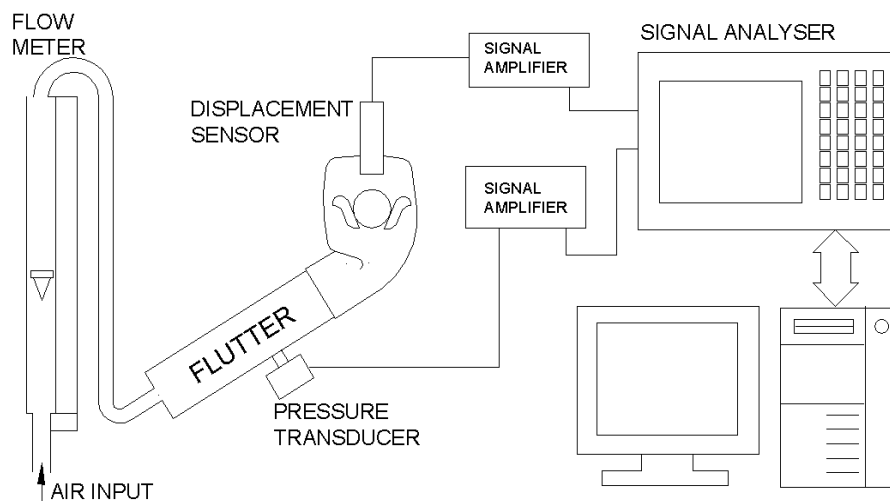


Figure 9. Experimental set-up and measurement system.

Experiments were made with airflow rates, Q , ranging between 2 and 8 m³/h, which is the range of airflow rate that a human being is able to produce. The entrance tubing in the Flutter makes a 30° angle to the horizontal position. This way, the air outlet tube, that contains the conical section and the sphere, keeps the vertical position.

The following figures show experimental results on the measurements of the vertical vibration of the sphere and the pressure inside the entrance tubing, for air flow rates of 2.0, 3.8 and 6.0 m³/h. Time signals represent a single sample and the spectra results from an average procedure of 10 samples.

As can be seen in “Figure 10”, time domain signals of displacement and pressure present a periodic nature which is apparent by the presence of a fundamental frequency and its higher order harmonics and also by the indicative modulation in amplitude.

There is strong correlation between signals $x(t)$ and $p(t)$ and this is confirmed by calculation of the coherence function $\gamma_{xp}^2(f)$, whose values resulted almost equal to unity for

the analyzed frequencies band (0 - 500 Hz). The only value less than unity value presented in Figure 10 indicates the presence of an electromagnetic interference at $f = 60$ Hz.

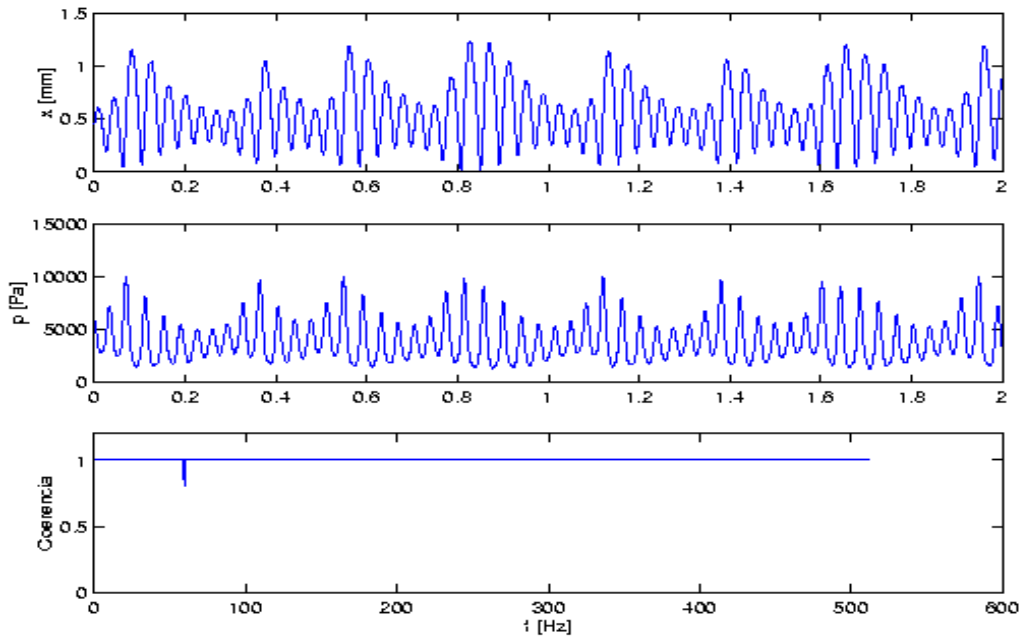


Figure 10. Displacement $x(t)$, input pressure $p(t)$ and coherence function for $Q = 2.0 \text{ m}^3/\text{h}$.

The spectra of the signals obtained for $Q = 2.0 \text{ m}^3/\text{h}$ are shown in “Figure 11”, where the large peak is the fundamental frequency and the lower ones present a frequency spacing of 4.125 Hz, indicating an amplitude modulation.

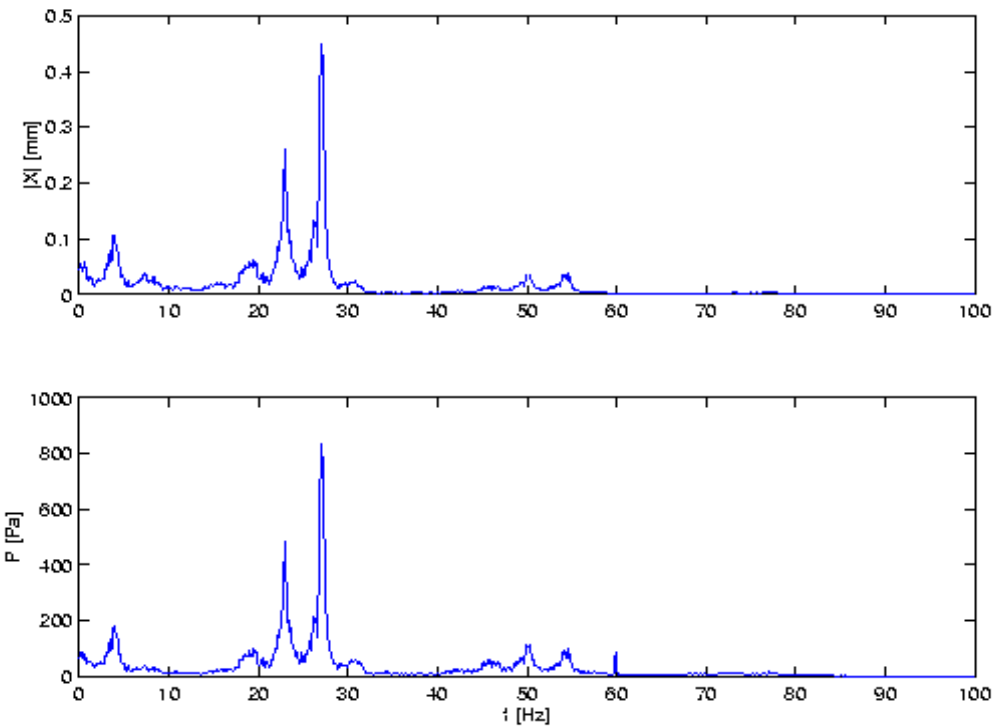


Figure 11. Spectra of x and p , for $Q = 2.0 \text{ m}^3/\text{h}$

In the time domain, for airflow rates less than $5 \text{ m}^3/\text{h}$ it is observed a strong modulation in amplitude on the vibration and on the pressure signals. The intensity of the modulation goes falling until an airflow rate of $6 \text{ m}^3/\text{h}$ and after that practically it disappears, indicating therefore, a transition on the behavior of the dynamic system. On the frequency spectra of the inlet pressure this modulation can be confirmed by the presence of lateral bands around the fundamental frequency and its harmonics, as can be seen in “Figure 12”.

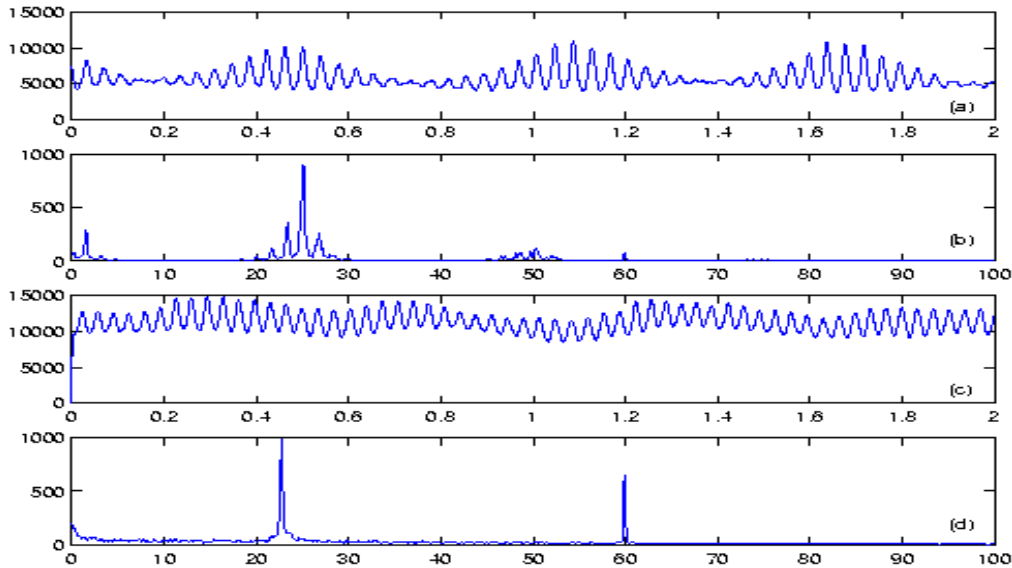


Figure 12. Comparison of the pressure signals $p(t)$ and $|P(f)|$ for $Q = 3.8 \text{ m}^3/\text{h}$ in (a) , (b) and for $Q = 6.0 \text{ m}^3/\text{h}$ in (c) , (d).

The same behavior is found in the sphere vibration signals. They are not shown here, considering that the coherence of $x(t)$ and $p(t)$ is equal to one.

The fundamental or carrier frequency and its lateral frequency bands vary with the imposed air flow rate in the entrance of the Flutter. According to “Table 1”, it can be observed a small reduction in the fundamental frequency (f_p) and in the modulation frequency (B_f) with the increase in the airflow rate.

Table 1. Fundamental frequency and the lateral bands as function of airflow rate.

Q	[m^3/h]	2.000	3.000	3.800	5.000	7.800
f_p	[Hz]	27.125	27.250	25.125	25.375	24.5
B_f	[Hz]	4.125	3.625	1.750	1.500	-0-

A visual observation of sphere did show that for higher airflow rates its movement is basically vertical and there is no occurrence of shocks of the sphere with the conical wall of the Flutter. In other situations, mainly for lower flow rates, between 2 and $3.8 \text{ m}^3/\text{h}$, the sphere rotates and translates in the vertical and horizontal directions, touching the conical wall, promoting the existence of the low frequency modulation on the sphere vibration. This behavior is not considered in the present computational model and this hinders its confirmations on the simulation results.

Other preliminary experiments were conducted, changing the orientation of the inlet tubing. For these situations the sphere motions are similar to those obtained for low flow

rates. Even using the maximum flow rate allowed by the feeding compressor it was not possible to achieve the stabilization of the sphere vibrations. The cause of this behavior can be explained by the constant presence of shocks of the sphere against the conical wall.

4. CONCLUSIONS

A novel device (Flutter) for respiratory physiotherapy was dynamically investigated in this study. Based on a numerical simulation and a theoretical modeling it was possible to study the influence of parameters such as air inflow velocity, on the aerodynamic lift force, on the vibration of the sphere, and on the inlet pressure fluctuations.

The flow rate $Q = 2.0 \text{ m}^3/\text{h}$ was used to compare the experimental results with those obtained by the adopted computational model. In this situation, the x mean values and their variation ranges, result equal to $0.62 : (0.18 - 1.3) \text{ mm}$ for the simulated case, and $0.56 : (0.06 - 1.24) \text{ mm}$, for experimental test, corresponding to a +10.7% difference. The simulated and experimental fundamental frequencies are equal to 29.3 Hz and 27.125, corresponding to a difference of 8.01 %. Despite these acceptable errors, it is not possible to extend, at the present stage of this research, the application of the computational model for flow rate values greater than $2.0 \text{ m}^3/\text{h}$, until new simulations tests were completed.

This simplified dynamic model can not handle with the sphere lateral and rolling motions and with the sphere impacts on the surface of the cone, which are important effects observed in the experiments.

The experimental set-up furnished displacement and pressure time signals and the corresponding power spectra. For the situation where the mouthpiece of the “Flutter” was kept horizontal, preliminary results demonstrated that the fundamental oscillations frequency of the sphere and its harmonics also depend on the airflow rate.

The effectiveness of the Flutter to improve sputum elimination in patients is eventually most present when the modulating frequency, present on the sphere motion and on the inlet pressure, has a value close to some of the natural frequencies of the lungs and bronchi.

The experiments had shown that only for flow rate values around $3.8 \text{ m}^3/\text{h}$, the modulation intensity is significant, indicating that greater flow rates will not produce the desired effect on the patient.

5. ACKNOWLEDGEMENTS

The authors F.P. Lépure Neto and L.C. De Lima gratefully acknowledge grants provided by CNPq. They also thank Prof. O. S. Hernandez (UFU) for providing instrumentation support such as pressure transducer, amplifier and rotameter.

6. REFERENCES

- Lauder, B.E. and Spalding, D.B., 1974 *The Numerical Computation of Turbulent Flows*, Computer Methods in Applied Mechanics and Engineering, vol. 3, pp. 269-289.
- Lindermann, H., 1992 *Zum Stellenwert der Physiotherapie mit dem VRP1-Desitin (“Flutter”)*, Pneumologie, vol. 46, pp. 626-630.